Electronic Supplementary Information (ESI)

Facile Synthesis of a Water Stable 3D Eu-MOF Showing High Proton Conductivity and Sensitive Luminescence Sensor for Cu^{2+} Ions

Xin Wang,[1] Tao Qin,[1] Song-Song Bao,[2] Yu-Chi Zhang,[1] Xuan Shen,[1] Li-Min Zheng,[2] and Dunru Zhu*,[1,2]

[1]State Key Laboratory of Materials-Oriented Chemical Engineering, College of Chemical Engineering, Nanjing Tech University, Nanjing, 210009, P. R. China

[2]State Key Laboratory of Coordination Chemistry, Nanjing University, Nanjing 210093, P. R. China

Contents

Experimental Section

1. General Remarks

All chemicals were of analytical grade and used as received. Elemental analyses (C, H, N) were carried out with a Thermo Finnigan Flash 1112A elemental analyzer. FT-IR spectrum was recorded on a Nicolet 380 FT-IR instrument (KBr discs) in the 4,000–400 cm^{-1} region. Thermogravimetric analysis (TGA) was performed on a NETZSCH

STA 449C thermal analyzer under nitrogen atmosphere at a scan rate of 10°C/min. Powder X-ray diffraction patterns (PXRD) were measured using a Bruker AXS D8 Advance powder diffractometer at 40 kV, 40 mA for Cu K_α (λ = 1.5406 Å), with a scan speed of 0.2 s/step and a step size of 0.02°. The gas sorption experiment was performed by using a Micromeritics 3500 automated micropore gas analyzer.

2. Single Crystal Growth of 1

A mixture of $Eu(NO_3)_3 \cdot 6H_2O$ (0.0452 g, 0.1 mmol), 3,3'-dimethoxy-4,4'-biphenyldicarboxylic acid (H_2L) (0.0309 g, 0.1 mmol), $H_2C_2O_4 \cdot 2H_2O$ (0.0126 g, 0.1 mmol), DMF (2 mL) and H_2O (0.7 mL) was heated at 120°C in a 25 mL capacity stainless-steel reactor with a Teflon-lined for 2 days and then cooled to room temperature. Several colorless block crystals of **1** were obtained.

3. Crystal Structure Determination

Diffraction data for **1** were collected on a Bruker Smart APEX II CCD diffractometer with graphite-monochromated Mo-K_α radiation (λ = 0.71073 Å). Multi-scan corrections were applied by using the SADABS program.[1] The structure was solved by direct methods and refined by the full-matrix least-squares based on F^2 using SHELXTL-97 program.[2] All non-H atoms were refined anisotropically. The H atoms were added according to the ideal geometry and not refined. The crystal data and structure refinements of **1** are summarized in Table S1. Selected bond lengths and angles are listed in Table S2. CCDC-1012765 (**1**) contain the supplementary crystallographic data for this paper. These data can be obtained free of charge from The Cambridge Crystallographic Data Centre via www.ccdc.cam.ac.uk/data_request/cif.

Table S1 Crystal data and structure refinements for **1**

Empirical formula	$C_6H_{16}EuNO_{12}$
Formula weight	446.16
T (K)	296(2)
Crystal system	Monoclinic

Space group	$P2_1/n$
a (Å)	9.6706(10)
b (Å)	11.7551(13)
c (Å)	12.3115(13)
β (°)	99.2690(10)
V (Å^3)	1381.3(3)
Z	4
ρ_{calcd} (g cm^{-3})	2.145
μ (mm^{-1})	4.601
F (000)	872
Reflection collected	9869
Unique reflections	2565 [R_{int} = 0.0576]
GOF on F^2	0.985
R_1/wR_2 [$I > 2\sigma(I)$]	0.0313/0.0543
R_1/wR_2 (all data)	0.0513/0.0584

Table S2 Selected bond lengths (Å) and angles (°) for **1**

Eu1–O1	2.470(2)	Eu1–O1W	2.502(2)
Eu1–O2	2.413(2)	Eu1–O5	2.432(2)
Eu1–O7	2.482(3)	Eu1–O3^{ii}	2.469(3)
Eu1–O4^{ii}	2.427(2)	Eu1–O8^{iii}	2.466(2)
Eu1–O6^{i}	2.467(2)	Eu1–Eu1^{i}	6.3340(6)
Eu1–Eu1^{iii}	6.3781(6)	Eu1–Eu1^{iv}	6.2812(7)
O1–Eu1–O1W	82.31(8)	O1–Eu1–O2	66.66(8)
O1–Eu1–O3^{ii}	137.70(8)	O1–Eu1–O4^{ii}	143.92(9)
O1–Eu1–O5	82.58(9)	O1–Eu1–O6^{i}	72.63(8)
O1–Eu1–O7	136.11(8)	O1–Eu1–O8^{iii}	73.57(8)
O1W–Eu1–O2	71.42(8)	O1W–Eu1–O3^{ii}	74.07(8)
O1W–Eu1–O4^{ii}	81.91(8)	O1W–Eu1–O5	132.71(8)
O1W–Eu1–O6^{i}	66.91(8)	O1W–Eu1–O7	140.74(8)
O1W–Eu1–O8^{iii}	141.22(8)	O2–Eu1–O3^{ii}	72.69(8)
O2–Eu1–O4^{ii}	136.12(8)	O2–Eu1–O5	138.77(8)
O2–Eu1–O6^{i}	124.35(8)	O2–Eu1–O7	111.71(9)
O2–Eu1–O8^{iii}	71.28(8)	O3^{ii}–Eu1–O4^{ii}	66.71(8)
O3^{ii}–Eu1–O5	138.65(8)	O3^{ii}–Eu1–O6^{i}	125.50(8)
O3^{ii}–Eu1–O7	70.24(9)	O3^{ii}–Eu1–O8^{iii}	104.30(9)
O4^{ii}–Eu1–O5	84.69(8)	O4^{ii}–Eu1–O6^{i}	71.35(8)
O4^{ii}–Eu1–O7	69.47(8)	O4^{ii}–Eu1–O8^{iii}	134.14(8)
O5–Eu1–O6^{i}	65.83(8)	O5–Eu1–O7	72.06(9)
O5–Eu1–O8^{iii}	74.19(9)	O6^{i}–Eu1–O7	123.93(8)

Symmetry codes: i) 1-x, 2-y, -z; ii) 1/2-x, y-1/2, 1/2-z; iii) -x, 2-y, -z; iv) 1/2-x, y+1/2, 1/2-z.

Table S3 Side lengths and angles in hexagonal rings a and b

Ring	Distances (Å)		Angles (°)	
a	Eu1···Eu1^{i}	6.3440(6)	Eu1^{i}–Eu1–Eu1^{v}	105.8(1)
	Eu1^{i}···Eu1^{ii}	6.2812(7)	Eu1^{i}–Eu1^{ii}–Eu1^{iii}	138.7(1)
			Eu1–Eu1^{i}–Eu1^{ii}	112.4(1)
b	Eu1···Eu1^{vi}	6.3781(6)	Eu1^{v}–Eu1–Eu1^{vi}	91.4(1)
	Eu1^{vi}···Eu^{vii}	6.2812(7)	Eu1–Eu1^{v}–Eu1^{iv}	138.7(1)
			Eu1–Eu1^{vi}–Eu1^{vii}	97.6(1)

Symmetry codes: i) 1-*x*, 2-*y*, -*z*; ii) 1/2+*x*, 5/2-*y*, *z*-1/2; iii) 1-*x*, 3-*y*, -*z*; iv) *x*, 1+*y*, *z*; v) 1/2-*x*, 1/2+*y*, 1/2-*z*; vi) -*x*, 2-*y*, -*z*; vii) *x*-1/2, 5/2-*y*, *z*-1/2.

Table S4. Hydrogen-bonding geometry (Å, °) for **1**

D–H···A	d(D–H)	d(H···A)	d(D···A)	∠D–H···A
O1W–H1WA···O2W^{i}	0.85	1.92	2.754(4)	166
N1–H1A···O1W	0.90	2.51	3.076(5)	121
N1–H1A···O6^{ii}	0.90	2.00	2.875(4)	163
N1–H1B···O3W^{i}	0.90	1.87	2.760(5)	169
O1W–H1WB···O2W	0.85	2.14	2.876(4)	144
O2W–H2WA···O7^{iii}	0.85	2.27	3.012(3)	145
O2W–H2WA···O8^{iii}	0.85	2.42	3.075(4)	134
O2W–H2WB···O4W^{iv}	0.85	2.52	3.326(5)	158
O3W–H3WA···O4W^{iv}	0.85	1.98	2.812(5)	164
O3W–H3WB···O3^{v}	0.85	2.19	2.831(4)	132
O4W–H4WA···O1^{v}	0.85	2.22	2.941(5)	142
O4W–H4WB···O4^{iv}	0.85	2.09	2.893(4)	158
C6–H6B···O2^{vi}	0.96	2.51	3.267(6)	136

Symmetry codes: i) 1-*x*, 2-*y*, 1-*z*; ii) 1-*x*, 2-*y*, -*z*; iii) 1/2-*x*, 1/2+*y*, 1/2-*z*; iv) -*x*, 2-*y*, 1-*z*; v) 1/2-*x*, *y*-1/2,1/2-*z*; vi) 1+*x*, *y*, *z*.

4. Coordination Mode of Ox^{2-} Ligand, Molecular Structures and Hydrogen Bonds

Scheme S1. Coordination mode of oxalate ligand in **1**

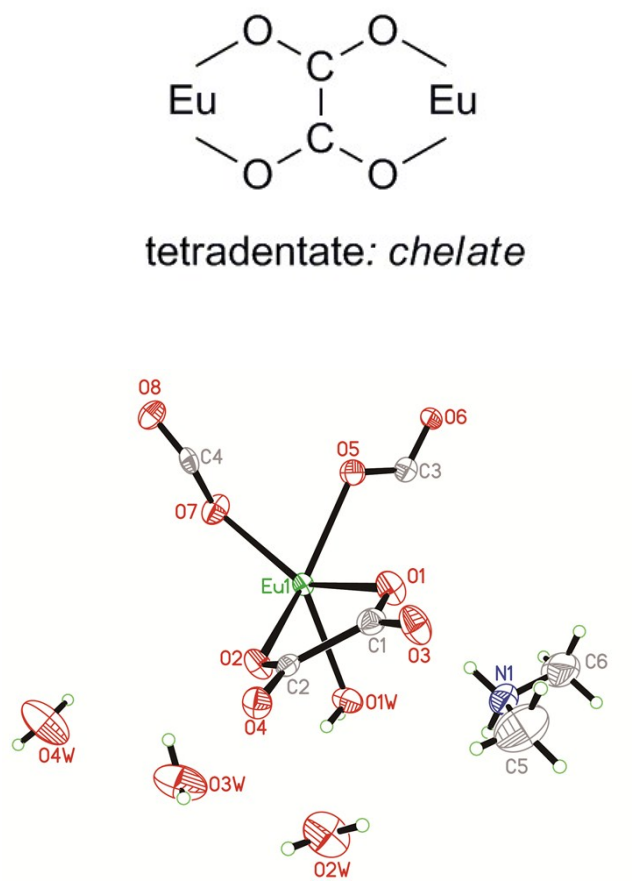

Fig. S1 ORTEP drawing (at 50% probability) of the asymmetric unit for **1**.

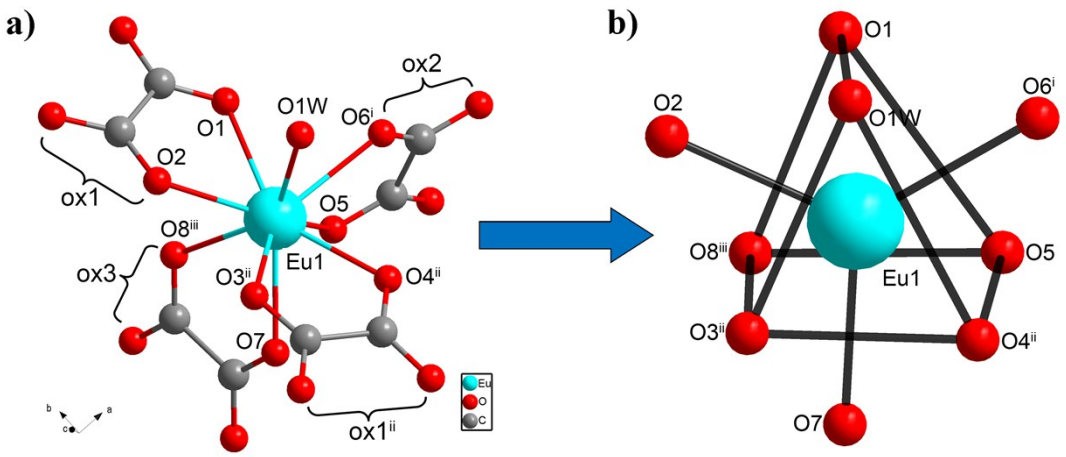

Fig. S2 a) Coordinated environment of Eu(III) ion in **1**. b) Tricapped trigonal prism of [EuO_9] unit. Symmetry codes: i) 1-*x*, 2-*y*, -*z*; ii) 1/2-*x*, *y*-1/2, 1/2-*z*; iii) -*x*, 2-*y*, -*z*.

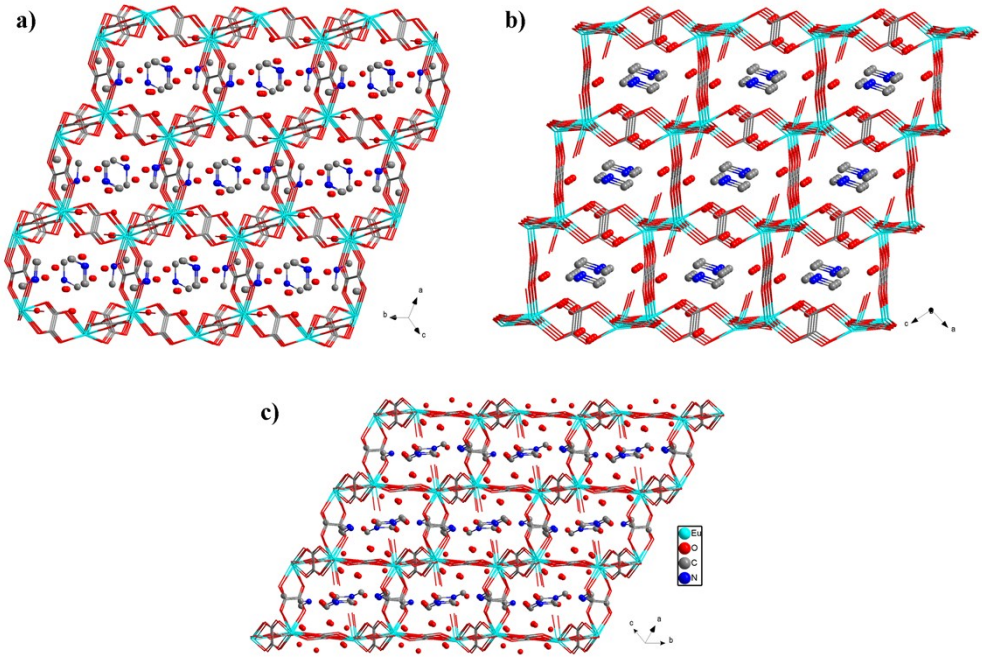

Fig. S3 The irregular 1D channels containing the $[Me_2NH_2]^+$ cation and lattice water molecules in **1** along different directions.

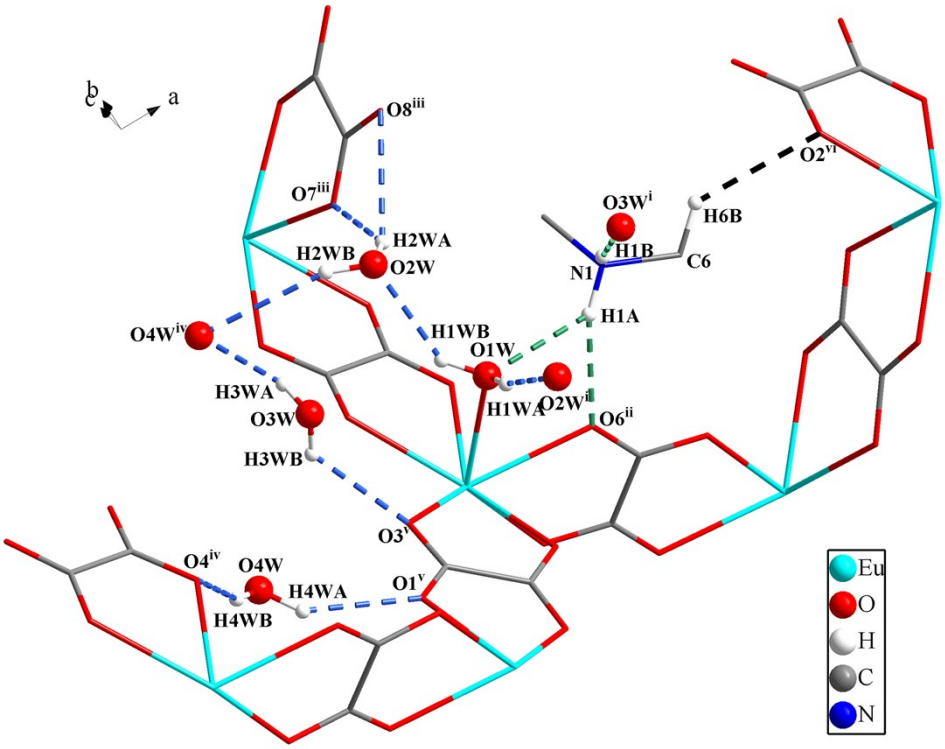

Fig. S4 An extensive hydrogen-bonded network in **1**.

5. The FT-IR Spectra

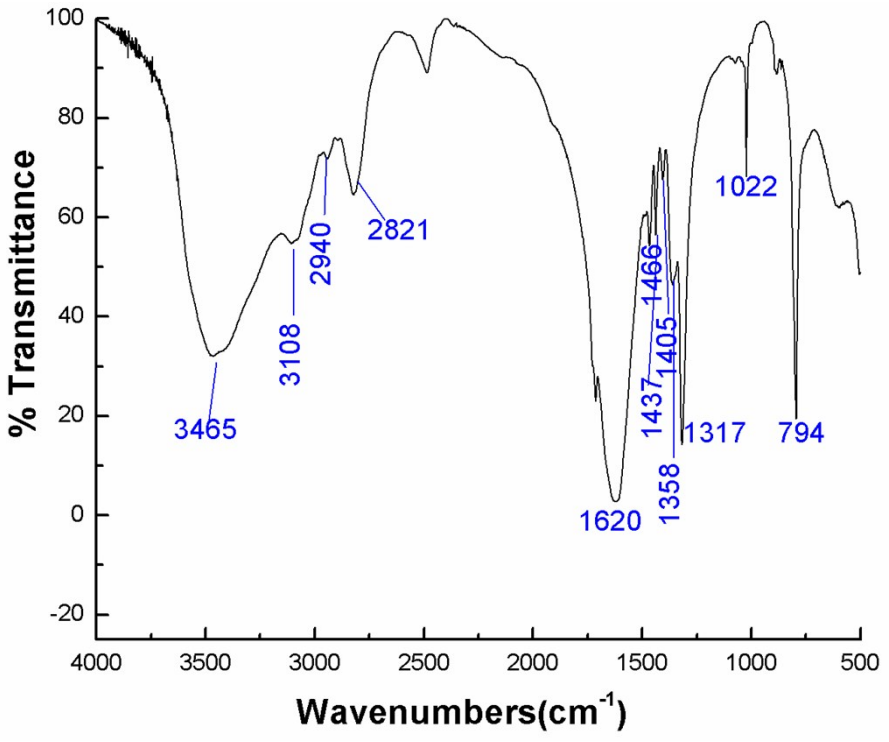

Fig. S5 FT-IR spectrum of **1**.

6. The PXRD Patterns

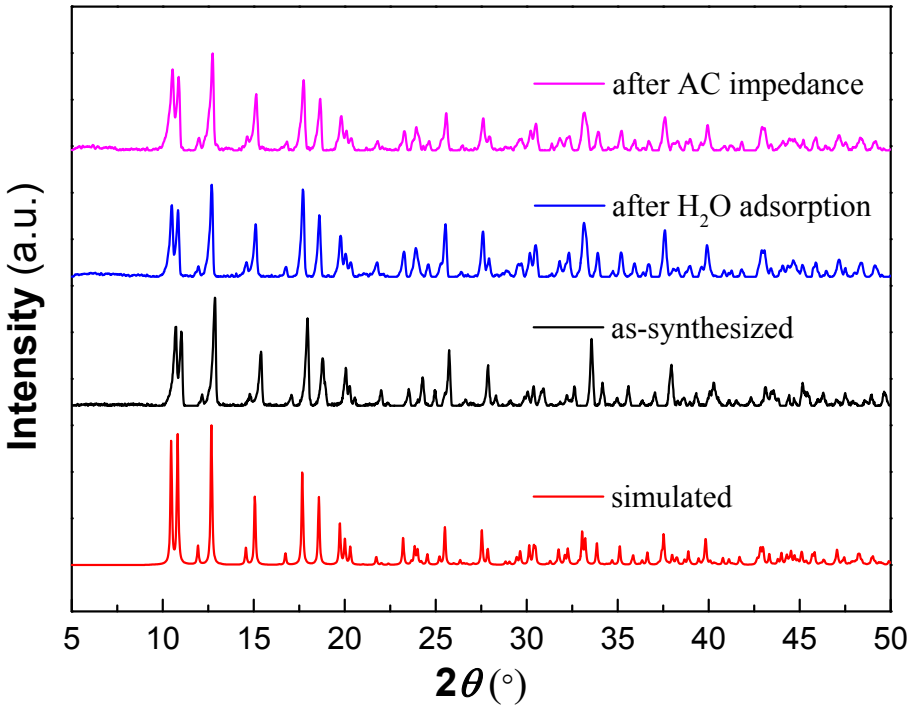

(a)

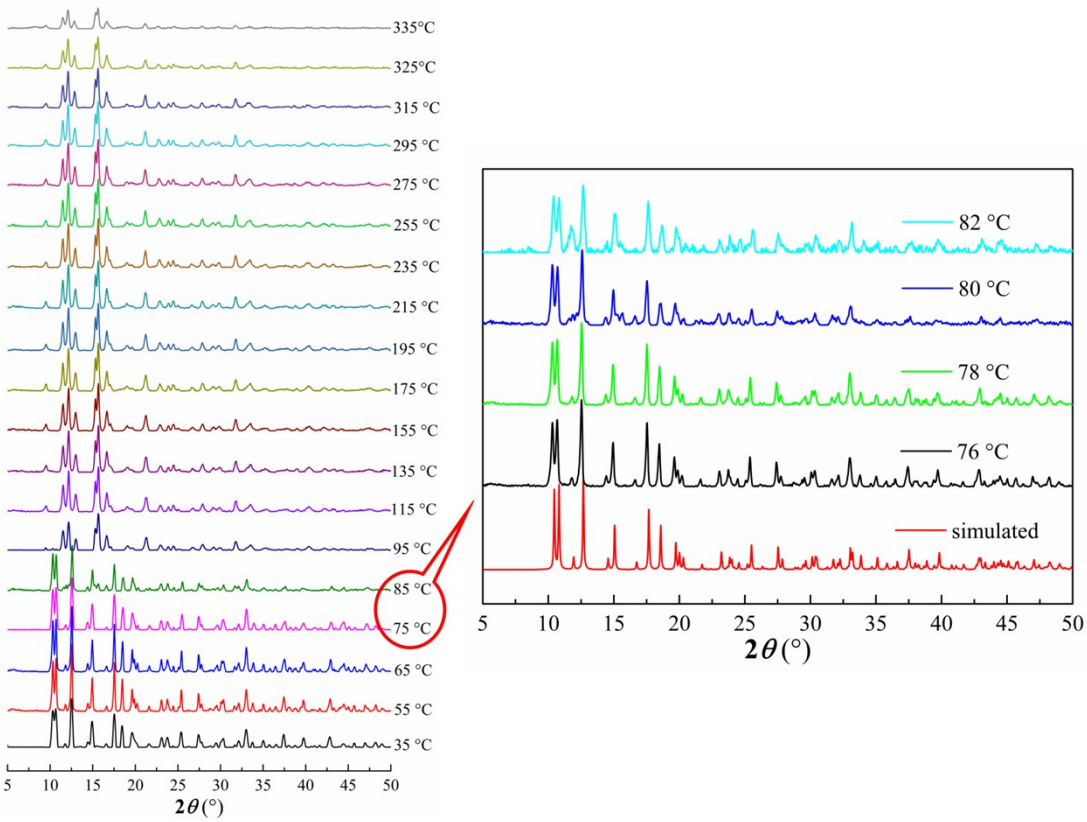

(b)

Fig. S6 (a) Experimental and simulated PXRD patterns of **1** and the PXRD patterns after water adsorption and AC impedance measurements. (b) The variable temperature PXRD patterns of **1**.

7. The Thermogravimetric Analysis

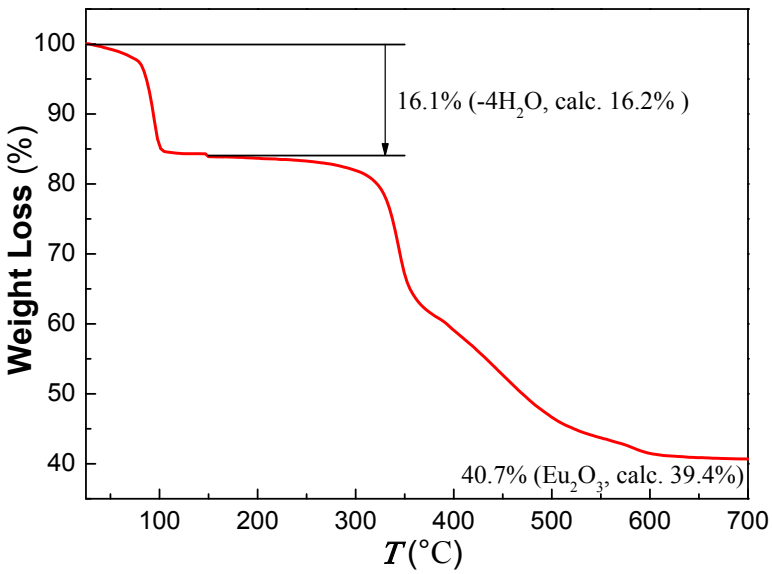

Fig. S7 TGA curve for **1**.

8. The Gas Sorption

The freshly prepared samples of **1** (160 mg) were first activated at room temperature overnight and then at 40°C for 4 hours to obtain the fully evacuated frameworks for the gas sorption test.

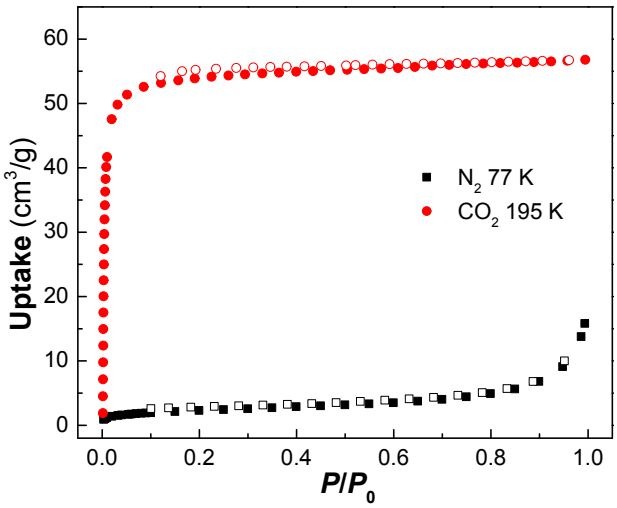

Fig. S8 The CO_2 (195 K) and N_2 (77 K) sorption isotherms for **1**. Solid symbols: adsorption; open symbols: desorption.

9. Impedance analyses

Humidity control: For impedance analysis, exposure of the sample to humid environments was performed for conditions at and below 95%RH using an Espec Corp. SH-221 humidity control oven. The temperature was also controlled by this oven form 15 to 55°C.

Impedance analysis: AC conductivities of **1** were measured using a sample pellet (2.5 mmϕ with a thickness of 0.62 mm), prepared under a pressure of ~1.2 GPa. Both round faces of the sample pellet were treated with gold paste and then the pellet was pressed in between parallel circular titanium electrodes in specially designed porous quartz cells. In general, the impedance measurements were carried out under multiple different environmental conditions by the conventional quasi-four-probe method, using gold paste and gold wires (50 μmϕ) with a Solartron SI 1260 Impedance/Gain-Phase Analyzer and 1296 Dielectric Interface in the frequency range of 1 MHz–1 Hz.

Data points were taken after the samples appearing to be equilibrated, with no deviation within one hour; this took on the order of half day per point.

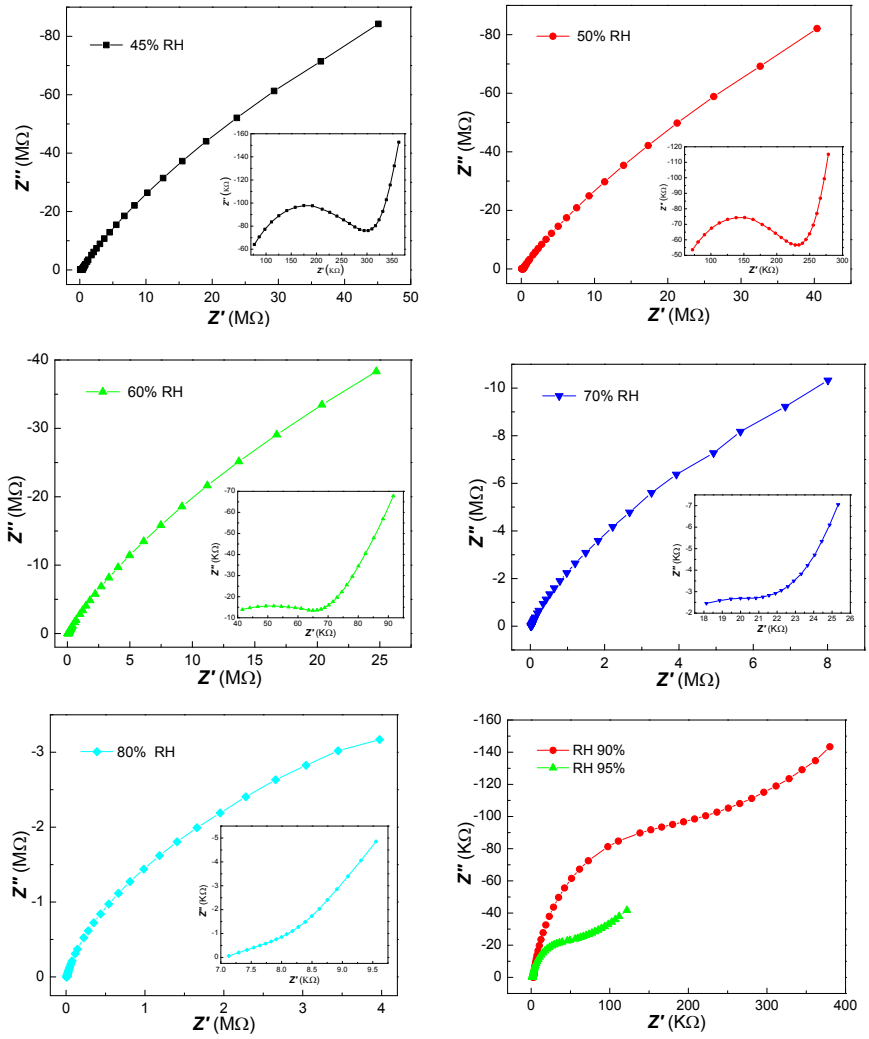

Fig. S9. Nyquist plots for **1** at 25°C and under varying RH from 45 to 95%.

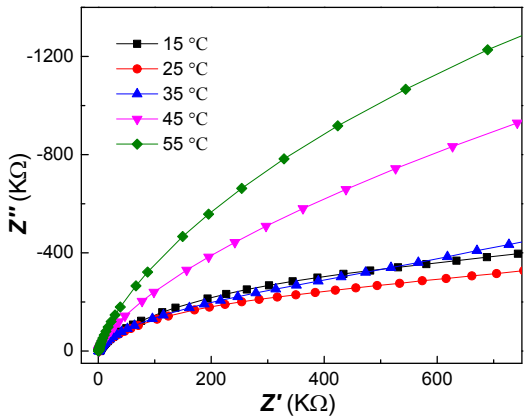

Fig. S10. Nyquist plots for **1** at 95% RH and various temperatures (°C).

Table S5. List of Proton Conductivities Ranked in Descending Order (below 100°C)

Compounds	σ (S/cm)	E_a (eV)	T (°C)	**RH** (%)
UiO-66$(SO_3H)_2$[3]	8.4×10^{-2}	0.32	80	90
TfOH@MIL-101[4]	8×10^{-2}	0.18	60	15
$Fe(THO)\cdot Fe(SO_4)(Me_2NH_2)_3$[5]	5×10^{-2}	0.24	25	98
$\{[(Me_2NH_2)_3(SO_4)]_2[Zn_2(ox)_3]\}$[6]	4.2×10^{-2}		25	98
PCMOF10[7]	3.55×10^{-2}	0.40	70	95
H^+@$Ni_2(dobdc)(H_2O)_2$ (pH = 1.8)[8]	2.2×10^{-2}	0.14	80	95
PCMOF2$^1/_2$[9]	2.1×10^{-2}	0.21	85	90
H^+@$Ni_2(dobdc)(H_2O)_2$ (pH = 2.4)[8]	1.9×10^{-2}	0.12	80	95
$La(H_5DTMP)\cdot 7H_2O$[10]	8×10^{-3}	0.25	24	98
$(NH_4)_2(H_2adp)[Zn_2(ox)_3]\cdot 3H_2O$[11]	8×10^{-3}	0.63	62	98
Ca-PiPhtA-NH_3[12]	6.6×10^{-3}	0.4	25	98
PCMOF-5[13]	4×10^{-3}	0.16	28	98
Cu-TCPP nanosheet[14]	3.9×10^{-3}	0.28	25	98
Cd-5TIA[15]	3.61×10^{-3}	0.16	28	98
In-IA-2D-1[16]	3.4×10^{-3}	0.61	27	98
Sulfonated MIL-53(Al)[17]	$\sim3\times10^{-3}$	NA	~65	<10
$[Me_2NH_2][Eu(ox)_2(H_2O)]$[this work]	2.73×10^{-3}	0.398	55	95
$V^{II}[Cr^{III}(CN)_6]_{2/3}\cdot 4.2H_2O$[18]	2.6×10^{-3}	0.10, 0.19	50	100
$[\{(Zn_{0.25})_8(O)\}Zn_6(L)_{12}(H_2O)_{29}(DMF)_{69}(NO_3)_2]_n$[19]	2.3×10^{-3}	0.22	25	95
$(NH_4)_4[MnCr_2(ox)_6]\cdot 4H_2O$[20]	1.7×10^{-3}	0.23	40	96
$Co^{II}[Cr^{III}(CN)_6]_{2/3}\cdot 4.8H_2O$[18]	1.7×10^{-3}	0.22	35	100
$MgH_6ODTMP\cdot 6H_2O$[21]	1.6×10^{-3}	0.31	19	100
β-PCMOF2[9]	1.3×10^{-3}	0.28	85	90
$Fe(ox)\cdot 2H_2O$[22]	1.3×10^{-3}	0.37	25	98
$\{[Ca(D\text{-}Hpmpc)(H_2O)_2]\cdot 2HO_{0.5}\}_n$[23]	8.9×10^{-4}	0.21	60	97
Ca-PiPhtA-I[12]	5.7×10^{-4}	0.23	24	98
In-IA-2D-2[16]	4.2×10^{-4}	0.48	27	98
GdHPA-II[24]	3.2×10^{-4}	0.23	21	98
$[Co^{III}La^{III}(notpH)(H_2O)_6]ClO_4\cdot 5H_2O$ (CoLa-II-SC)[25]	3.05×10^{-4}	0.42	25	95
Ca-BTC-H_2O[26]	1.2×10^{-4}	0.18	25	98
$K_2(H_2adp)[Zn_2(ox)_3]\cdot 3H_2O$[27]	1.2×10^{-4}	0.45	25	98
$\{NH(prol)_3\}[MCr(ox)_3]$[28]	1.0×10^{-4}	NA	25	75
$Zr(O_3PCH_2)_2N\text{-}C_6H_{10}\text{-}N(O_3CH_2P)_2H_4\cdot 5.5H_2O$_lp[29]	1.0×10^{-4}	0.09, 0.23	80	95
$[NMe_3(CH_2CO_2H)][FeCr(ox)_3]\cdot nH_2O$[30]	8.0×10^{-5}	NA	25	65
In-5TIA[15]	5.35×10^{-5}	0.14	28	98
$[Zn(l\text{-}L_{Cl})(Cl)](H_2O)_2$[31]	4.45×10^{-5}	0.34	31	98
$[Zn(d\text{-}L_{Cl})(Cl)](H_2O)_2$[31]	4.42×10^{-5}	0.36	31	98
Sr-SBBA[32]	4.4×10^{-5}	0.56	25	98
$[H_3O][Co^{III}La^{III}(notp)(H_2O)_4]ClO_4\cdot 3H_2O$ (CoLa-III)[25]	4.24×10^{-5}	0.28	25	95
$\{Mn(DHBQ)(H_2O)_2\}\cdot 2H_2O$[33]	4.0×10^{-5}	0.26	RT	98
$(Me_2NH_2)_2[Li_2Zr(C_2O_4)_4]$[34]	3.9×10^{-5}	0.64	17	67

10. Luminescent property

Photoluminescence spectra were performed on a HITACHI F-7000 luminescence spectrometer. The solid state photoluminescence of **1** was investigated at room temperature with the excitation wavelength of 395 nm. In the metal ions-sensing study, all of the luminescence spectra were recorded in the same test conditions. For the experiments of sensing metal ions, powder of **1** (10 mg) was immersed in 10^{-2} M $M(NO_3)_x$ (M = Na^+, K^+, Mg^{2+}, Ca^{2+}, Zn^{2+}, Cd^{2+}, Pb^{2+} or Cu^{2+}) aqueous solutions (10 mL). Before photoluminescence measurements, the suspensions were oscillated for 10 min using ultrasonic waves to ensure uniform dispersion. The excitation wavelength of the suspensions was 259 nm, and the slit widths of excitation and emission spectra were 5 nm.

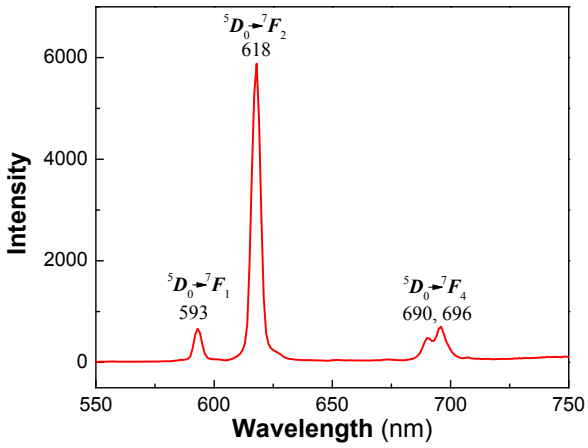

Fig. S11 The solid-state photoluminescence emission spectra of **1** at room temperature (λ_{ex} = 395 nm).

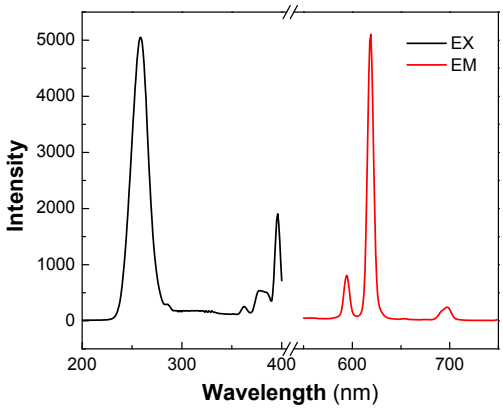

Fig. S12 The excitation (black) and photoluminescence spectra (red) of **1** powder

after suspension in aqueous solution at room temperature (excited and monitored at 259 nm and 619 nm, respectively).

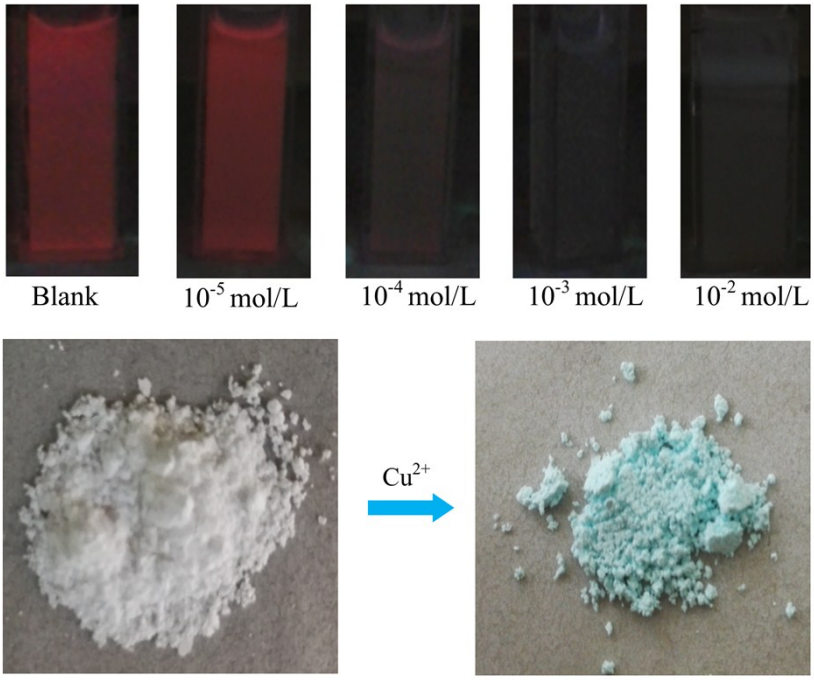

Fig. S13 Luminescence photographs of **1** powder after suspension in different concentrations of $Cu(NO_3)_2$ aqueous solution under UV light of 254 nm (top) and the photographs of **1** powder before and after immersion in 10^{-2} M $Cu(NO_3)_2$ aqueous solution.

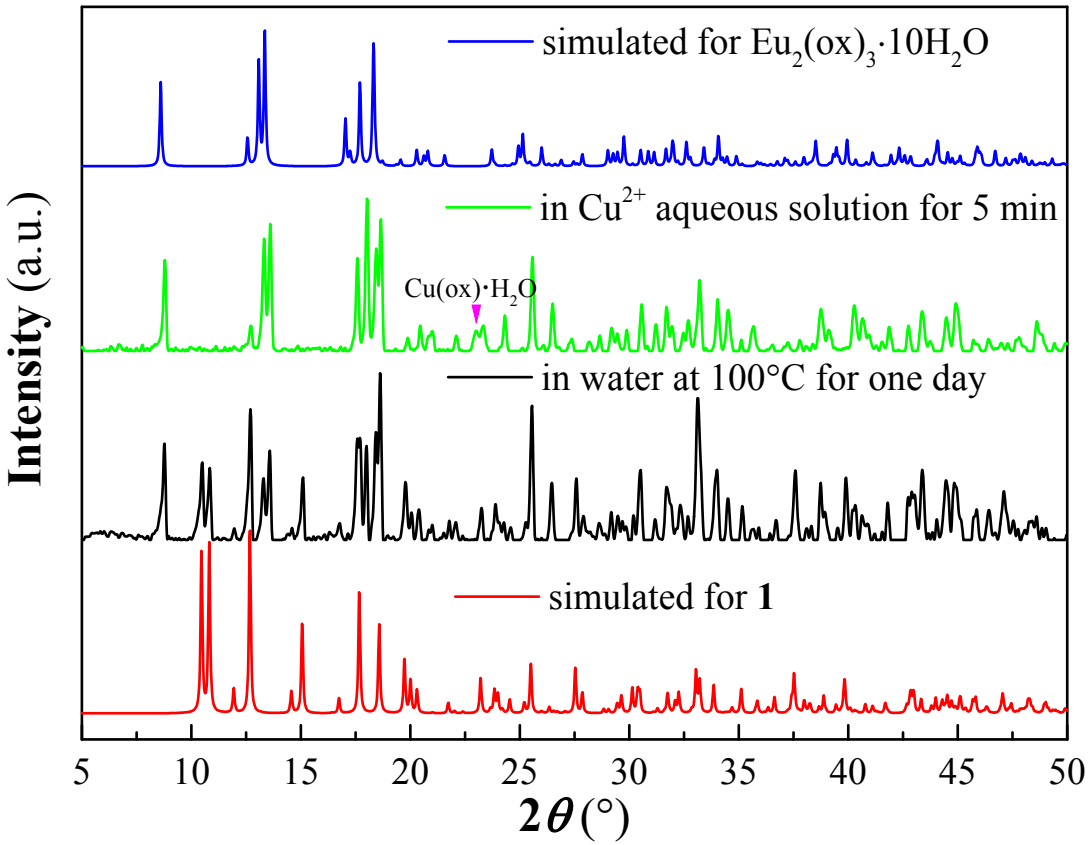

Fig. S14 The PXRD patterns of powder of **1** after immersed in 10^{-2} M $Cu(NO_3)_2$ aqueous solutions and a complete phase transition is observed by comparing with the simulated and the boiling water-treated samples of **1**.

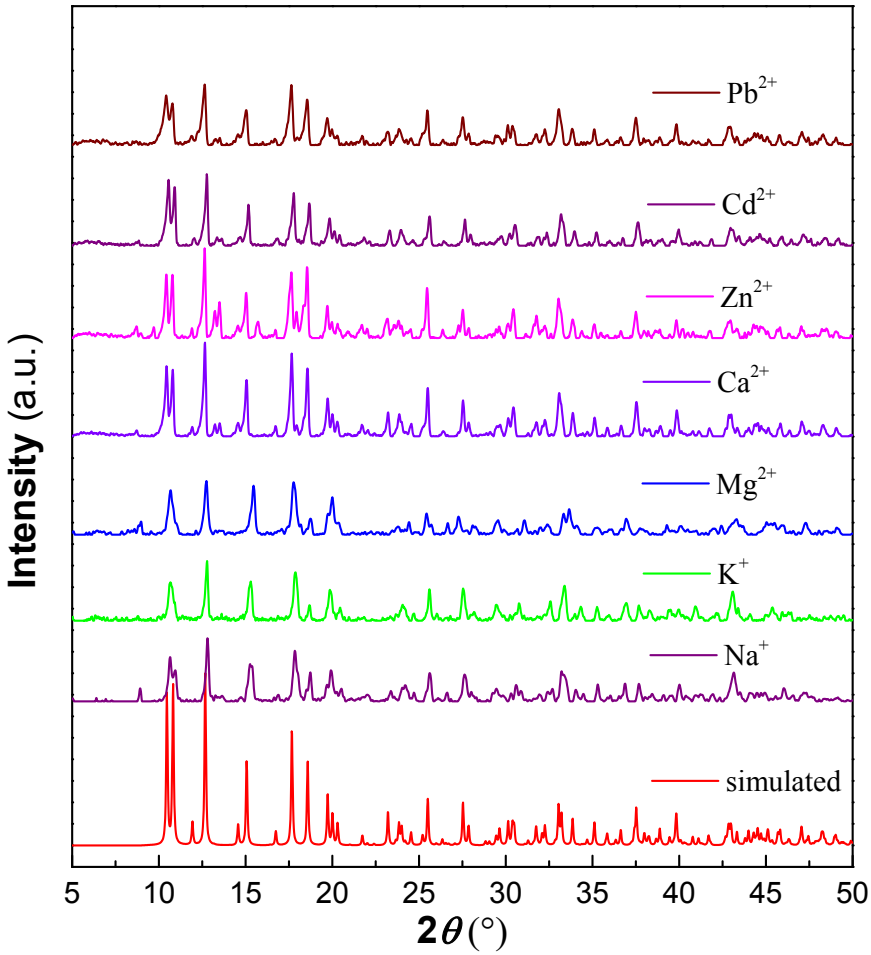

Fig. S15 The PXRD patterns of powder of **1** after immersed in different 10^{-2} M $M(NO_3)_x$ (M = Na^+, K^+, Mg^{2+}, Ca^{2+}, Zn^{2+}, Cd^{2+}, Pb^{2+}) aqueous solutions.

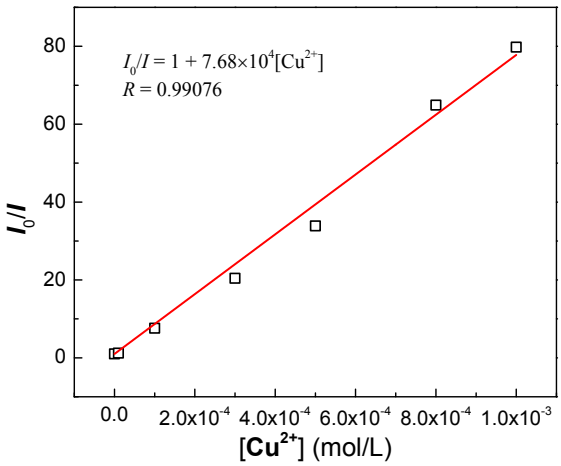

Fig. S16 Stern–Volmer plots of luminescence of **1** in the presence of Cu^{2+} ions.

References

[1] Bruker. *SADABS*, *SMART* and *SAINT*. Bruker AXS Inc., Madison, Wisconson, USA, **2002**.

[2] G. M. Sheldrick, *SHELXL-97, program for the refinement of the crystal structures*. University of Göttingen, Germany, **1997**.

[3] W. J. Phang, H. Jo, W. R. Lee, J. H. Song, K. Yoo, B. Kim and C. S. Hong, *Angew. Chem. Int. Ed.*, **2015**, *54*, 5142.

[4] D. N. Dybtsev, V. G. Ponomareva, S. B. Aliev, A. P. Chupakhin, M. R. Gallyamov, N. K.Moroz, B. A. Kolesov, K. A. Kovalenko, E. S. Shutova and V. P. Fedin, *ACS Appl. Mater. Interfaces* **2014**, *6*, 5161.

[5] N. T. T. Nguyen, H. Furukawa, F. Gándara, C. A. Trickett, H. M. Jeong, K. E. Cordova and O. M. Yaghi, *J. Am. Chem. Soc.*, **2015**, *137*, 15394.

[6] S. S. Nagarkar, S. M. Unni, A. Sharma, S. Kurungot and S. K. Ghosh, *Angew. Chem. Int. Ed.*, **2014**, *53*, 2638.

[7] P. Ramaswamy, N. E. Wong, B. S. Gelfand and G. K. H. Shimizu, *J. Am. Chem. Soc.,* **2015**, *137*, 7640.

[8] W. J. Phang, W. R. Lee, K. Yoo, D. W. Ryu, B. Kim and C. S. Hong, *Angew. Chem. Int. Ed.*, **2014**, *53*, 8383.

[9] S. Kim, K. W. Dawson, B. S. Gelfand, J. M. Taylor and G. K. Shimizu, *J. Am. Chem. Soc.*, **2013**, *135*, 963.

[10] R. M. P. Colodrero, P. Olivera-Pastor, E. R. Losilla, M. A. G. Aranda, L. Leon-Reina, M. Papadaki, A. C. McKinlay, R. l. E. Morris, K. D. Demadis and A. Cabeza, *Dalton Trans.*, **2012**, *41*, 4045.

[11] M. Sadakiyo, T. Yamada and H. Kitagawa, *J. Am. Chem. Soc.*, **2009**, *131*, 9906.

[12] M. Bazaga-Garcia, R. M. Colodrero, M. Papadaki, P. Garczarek, J. Zon, P. Olivera-Pastor, E. R. Losilla, L. Leon-Reina, M. A. Aranda, D. Choquesillo-Lazarte, K. D. Demadis and A. Cabeza, *J. Am. Chem. Soc.*, **2014**, *136*, 5731.

[13] J. M. Taylor, K. W. Dawson and G. K. Shimizu, *J. Am. Chem. Soc.*, **2013**, *135*, 1193.

[14] G. Xu, K. Otsubo, T. Yamada, S. Sakaida and H. Kitagawa, *J. Am. Chem. Soc.*, **2013**, *135*, 7438.

[15] T. Panda, T. Kundu and R. Banerjee, *Chem. Commun.*, **2012**, *48*, 5464.

[16] T. Panda, T. Kundu and R. Banerjee, *Chem. Commun.*, **2013**, 49, 6197.

[17] M. G. Goesten, J. Juan-Alcañiz, E. V. Ramos-Fernandez, K. B. S. S. Gupta, E. Stavitski, H. van Bekkum, J. Gascon and F. Kapteijn, *J. Catal.*, **2011**, *281*, 177.

[18] S. Ohkoshi, K. Nakagawa, K. Tomono, K. Imoto, Y. Tsunobuchi and H. Tokoro, *J. Am. Chem. Soc.*, **2010**, *132*, 6620.

[19] S. Sen, N. N. Nair, T. Yamada, H. Kitagawa and P. K. Bharadwaj, *J. Am. Chem. Soc.*, **2012**, *134*, 19432.

[20] E. Pardo, C. Train, G. Gontard, K. Boubekeur, O. Fabelo, H. Liu, B. Dkhil, F. Lloret, K. Nakagawa, H. Tokoro, S. Ohkoshi and M. Verdaguer, *J. Am. Chem. Soc.*, **2011**, *133*, 15328.

[21] R. M. Colodrero, P. Olivera-Pastor, E. R. Losilla, D. Hernandez-Alonso, M. A. Aranda, L. Leon-Reina, J. Rius, K. D. Demadis, B. Moreau, D. Villemin, M. Palomino, F. Rey and A. Cabeza, *Inorg. Chem.*, **2012**, *51*, 7689.
[22] T. Yamada, M. Sadakiyo and H. Kitagawa, *J. Am. Chem. Soc.*, **2009**, *131*, 3144.
[23] X. Liang, F. Zhang, W. Feng, X. Zou, C. Zhao, H. Na, C. Liu, F. Sun and G. Zhu, *Chem. Sci.*, **2013**, *4*, 983.
[24] R. M. P. Colodrero, K. E. Papathanasiou, N. Stavgianoudaki, P. Olivera-Pastor, E. R. Losilla, M. A. G. Aranda, L. León-Reina, J. Sanz, I. Sobrados, D. Choquesillo-Lazarte, J. M. García-Ruiz, P. Atienzar, F. Rey, K. D. Demadis and A. Cabeza, *Chem. Mater.*, **2012**, *24*,3780.
[25] S. S. Bao, K. Otsubo, J. M. Taylor, Z. Jiang, L. M. Zheng and H. Kitagawa, J. *Am. Chem. Soc.*, **2014**, *136*, 9292.
[26] A. Mallick, T. Kundu and R. Banerjee, *Chem. Commun.*, **2012**, *48*, 8829.
[27] M. Sadakiyo, T. Yamada and H. Kitagawa, *J. Am. Chem. Soc.*, **2014**, *136*, 13166.
[28] H. Okawa, A. Shigematsu, M. Sadakiyo, T. Miyagawa, K. Yoneda and M. Ohba, H. Kitagawa,, *J. Am. Chem. Soc.*, **2009**, *131*, 13516.
[29] F. Costantino, A. Donnadio and M. Casciola, *Inorg. Chem.*, **2012**, *51*, 6992.
[30] M. Sadakiyo, H. Ōkawa, A. Shigematsu, M. Ohba, T. Yamada and H. Kitagawa, *J. Am. Chem. Soc.*, **2012**, *134*, 5472.
[31] S. C. Sahoo, T. Kundu and R. Banerjee, *J. Am. Chem. Soc.*, **2011**, *133*, 17950.
[32] T. Kundu, S. C. Sahoo and R. Banerjee, *Chem. Commun*., **2012**, *48*, 4998.
[33] S. Morikawa, T. Yamada and H. Kitagawa, *Chem. Lett.*, **2009**, *38*, 654.
[34] S. Tominaka, François-Xavier Coudert, T. D. Dao, T. Nagao and A. K. Cheetham, *J. Am. Chem. Soc.*, **2015**, *137*, 6428.